

N O T I C E

THIS DOCUMENT HAS BEEN REPRODUCED FROM
MICROFICHE. ALTHOUGH IT IS RECOGNIZED THAT
CERTAIN PORTIONS ARE ILLEGIBLE, IT IS BEING RELEASED
IN THE INTEREST OF MAKING AVAILABLE AS MUCH
INFORMATION AS POSSIBLE

CR-166179

JOINT INSTITUTE FOR AERONAUTICS AND ACOUSTICS



STANFORD UNIVERSITY



AMES RESEARCH CENTER

su-JIAA TR-19

SOME OBSERVATIONS OF FLOW STRUCTURE IN MULTIPLE JET MIXING

A. Krothapalli, D. Baganoff,
and K. Karamcheti

STANFORD UNIVERSITY
Department of Aeronautics and Astronautics
Stanford, California 94305

(NASA-CR-166179) SOME OBSERVATIONS OF FLOW
STRUCTURE IN MULTIPLE JET MIXING (Stanford
Univ.) 10 p HC A02/MF A01 CSCI 200

N81-26417

Unclas
G3/34 24833

March 1979



JIAA TR-19

SOME OBSERVATIONS OF FLOW STRUCTURE
IN MULTIPLE JET MIXING

A. KROTHAPALLI, D. BAGANOFF,
AND K. KARAMCHETI

DEPARTMENT OF AERONAUTICS AND ASTRONAUTICS
STANFORD UNIVERSITY
STANFORD, CALIFORNIA 94305

Presented at the "Second Symposium on Turbulent Shear Flows," July 2-4,
1979, Imperial College, London, England.

MARCH 1979

The work here presented has been supported by The National Aeronautics and
Space Administration, Ames Research Center, under Grant NASA 2233.

SOME OBSERVATIONS OF FLOW STRUCTURE IN MULTIPLE JET MIXING

A. Krothapalli,* D. Baganoff,** K. Karamcheti†

Joint Institute for Aeronautics and Acoustics
Department of Aeronautics and Astronautics
Stanford University, Stanford, California 94305

ABSTRACT

Results of hot wire measurements in an incompressible jet issuing from an array of rectangular lobes, equally spaced with their small dimensions in a line, both as a free jet, and as a confined jet, are presented. The quantities measured include mean velocity and the Reynolds stress in the two central planes of the jet at stations covering up to 115 widths (small dimension of the lobe) downstream of the nozzle exit. Measurements are carried out in three parts: a) on a single rectangular free jet, b) on the same jet in a multiple free jet configuration, c) on the same jet in a multiple jet configuration with confining surfaces (two parallel plates are symmetrically placed perpendicular to long dimension of each lobe covering the entire flow field under consideration). In the case of a multiple free jet, the flow field for downstream distance x greater than $60D$ (D = width of a lobe) resembles that of a jet exiting from a two-dimensional nozzle with its short dimension being the long dimension of the lobe. The field of turbulence is found to be nearly isotropic in the plane containing the small dimension of the lobes for x greater than $60D$. In the case of a confined multiple jet, the flow field is observed to be nearly homogeneous and isotropic for x greater than $60D$.

NOMENCLATURE

AR = Aspect ratio (L/D)
D = Width (small dimension) of the lobe
L = Length (long dimension) of the lobe
 L_1 = Spacing between the plates
S = Spacing between the lobes
U = Mean velocity component in the X-direction
 U_c = Mean velocity component along the centerline of the jet in the X-direction
 U_o = Mean velocity component in the exit plane of the jet in the X-direction
 U_s = Mean velocity component of the secondary flow in the X-direction.

u = Fluctuation velocity component in the X-direction
 $u_{rms} = \sqrt{u^2}$ = rms velocity fluctuation in the X-direction
 $\tilde{u} = \sqrt{u^2}/U_c$ (normalized rms velocity fluctuation in the X-direction)
V = Mean velocity component in the Y-direction
 $v_{rms} = \sqrt{v^2}$ = rms velocity fluctuation in the Y-direction
 $\tilde{v} = \sqrt{v^2}/U_c$ (normalized rms velocity fluctuation in the Y-direction)
W = Mean velocity component in the Z-direction
w = Fluctuation velocity component in the Z-direction
 $w_{rms} = \sqrt{w^2}$ = rms velocity fluctuation in the Z-direction
 $\tilde{w} = \sqrt{w^2}/U_c$ (normalized rms velocity fluctuation in Z-direction)
 $\frac{uv}{\rho U_c}$ = Components of the turbulent shear stress tensor
X = Coordinate along the jet axis
Y = Coordinate along the small dimension of the lobe
 $Y_{1/2}$ = Local half width of the U profile along the Y axis
Z = Coordinate along the long dimension of the lobe
 $Z_{1/2}$ = Local half width of U profile along the Z-axis
 $\eta = Y/X$
 $\xi = Z/X$

INTRODUCTION

Multiple jets are used in a wide variety of engineering applications, for example, thrust augmenting ejectors for VTOL/STOL aircraft. The configuration of interest here is an array of rectangular lobes in a line as shown in Figure 1. Very few investigations have been reported in the literature regarding the structure and development of multiple jets, in particular the present configuration. Early work on this subject was done by Corrisin (1) who studied the flow from seven parallel slot nozzles in a common wall with emphasis on flow stabilization methods. Laurence and Benninghoff (2), and Laurence (3) studied the flow emanating from four rectangular lobes. Most of the emphasis in these studies was placed on finding a noise reducing mechanism rather than on the detailed structure of the flow field. The gross characteristics of

* Ph.D. Student.

** Professor.

† Professor and Director, JIAA.

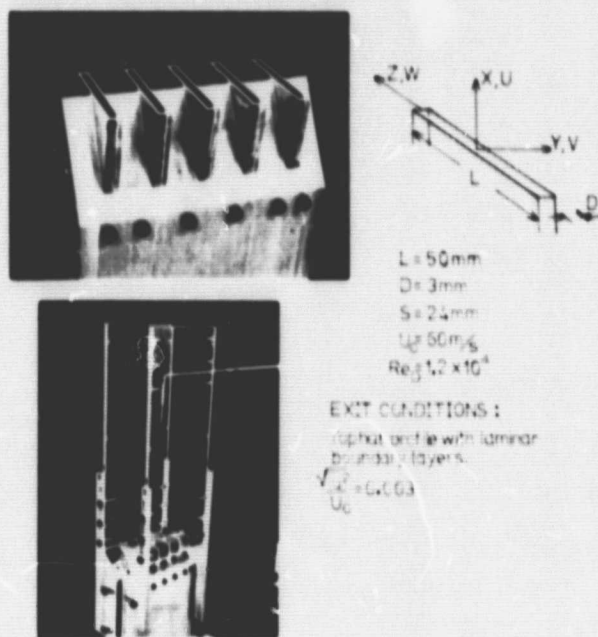


Fig. 1 Model and Definitions

the flow field emanating from rectangular lobes in line was recently reported by Marsters (4). The flow emanating from a series of closely spaced holes in line has been studied experimentally by Knystautas (5). Overall aerodynamic studies have been made by Aiken (6) on an ejector with multiple rectangular lobes with various spacing to width ratios and nozzle dimensions. In all the studies mentioned above, most of the measurements were made on mean flow rather than on the detailed turbulence structure. The purpose of the present paper is to present and discuss the results of experiments with a multiple jet configuration and thus add to the understanding of its fluid mechanical structure. The data also provide numerical analysts with a basis on which a computational model can be built. The experimental investigation presented here constitutes a part of a larger programme on turbulent mixing of multiple rectangular jets being studied at Stanford.

The characteristics of the flow field depend upon the aspect ratio of the lobe, inlet geometry of each lobe, the type of exit velocity profile for each lobe, the magnitude of the turbulence intensity at the exit plane of each lobe, the Reynolds number at the lobe exit, spacing between the lobes, configuration of confining surfaces and condition of the ambient medium into which the jet is issuing. In the present investigation, a lobe of aspect ratio 16.7 was chosen. The spacing between the lobes was 8D (D being the small dimension of the lobe). These parameters were chosen to be consistent with the nozzle used by Aiken (6). Inlet geometry of the nozzle was designed specifically to obtain a minimum turbulence level at the exit plane. The velocity profile at the exit plane of each lobe was flat with a laminar boundary layer at the walls. A mean velocity of 60 m/s was maintained at the exit plane of each lobe. This results in a Reynolds number of 1.2×10^4 based on the width of the lobe. Two parallel plates of 100 widths long were symmetrically placed perpendicular to the long dimension of the lobe as shown in Figure 1. The spacing between the plates can be adjusted between 1.2L to 1.7L (L being the long dimension of the lobe).

Measurements were made using hot-wire anemometry. They include the mean velocities and turbulent intensities for the three components of velocity and the turbulent shear stresses \overline{UV} and \overline{UW} (see Figure 1). Most of the detailed measurements were made in the two perpendicular central planes of the center lobe.

APPARATUS, INSTRUMENTATION AND PROCEDURE

A blow down air supply system was used to provide the airflow to a cylindrical settling chamber whose dimensions are 1.75 m long and 0.6 m in diameter. The facility is designed to provide sonic conditions at the exit plane of the nozzle for other experiments. Before reaching the nozzle, air passes through an adapter which contains six screens set 5 cm apart to reduce disturbances at the inlet of the nozzle. The ratio of areas between the adapter and the nozzle is 90, which is exceptionally large when compared with the contraction ratio for conventional wind tunnels. The turbulence level at the exit of the nozzle was about 0.3% at 60 m/sec. The long (L) and short (D) dimensions of the rectangular lobe exit are 50 mm and 3 mm respectively. The spacing (S) between the lobes is 24 mm. Each lobe exit is preceded by a 40 mm long rectangular (50 mm \times 3 mm) channel. The spacing (L₁) between the plates can be varied from 6 cm to 8.5 cm (see Figure 1). The experimental facility and the model are described in detail by Krothapalli (7). The exit velocity of the jet was maintained to an accuracy better than one percent.

Measurements were made with DISA 55M01 constant temperature anemometers in conjunction with DISA 55D10 linearizers. Most of the measurements were made using either an x-wire or a single wire. These wires were manufactured by DISA and constructed from 5 μ m platinum coated tungsten wire with an active length of 1.2 mm. When X-probes were used, each of the attenuators on the linearizers was adjusted to give the same output for each wire when the probe was perfectly aligned with the stream. The yaw sensitivity of each wire was then checked. The simple cosine law was used to decompose the velocities. From the calibration, the use of an x-wire probe in turbulent flows was found to be limited to situations where the angular rotation of the velocity vector does not exceed $\pm 25^\circ$. The response of the hot wire was assumed linear and no corrections resulting from higher order terms were applied.

The signals were then passed through two DISA type 55D31 digital voltmeters, DISA 55D35 rms units, and TSI model 1076 voltmeters to get the mean and rms values. The integration times on these instruments can be selected in discrete steps from 0.1 sec to 100 sec. Measurements of correlations were made using an HP 3712 A correlator. For most of the results presented random errors were estimated to be of the order of 2 to 3 percent, and a systematic error in the axial component of velocity (due to cosine law decomposition) of approximately 5 percent was present.

A Cartesian coordinate system (x,y,z) is chosen with its origin located at the center of the center lobe as shown in Figure 1, with the x axis oriented along the centerline of the jet. Hot wire traverses were made in the two central x,y and x,z planes at various streamwise (x) locations covering up to 115D. Unless otherwise stated, all the data presented here were taken with the x-wire probe. The experiment was conducted in three parts. In the first part, measurements were made on the center lobe with all the other lobes blocked. In the second part, measurements were made on the center lobe with all five lobes blowing. In the third part, measurements were again made on the

center lobe with all five lobes blowing and with confining surfaces in place. Most of the measurements in all the three cases were made on the two central planes of the center lobe. Mean velocity measurements were made across the center three jets in order to establish the symmetry of the flow about their central planes; however, only the data for each half plane of the center lobe will be presented.

RESULTS AND DISCUSSION

General Features of the Flow Field

On the basis of the present investigation and the results reported by Sforza et al. (8)(9), Sfeir (10)(11), and those summarized by Rajaratnam (12), the flow field of a rectangular free jet may be represented schematically as shown in Figure 2. Also

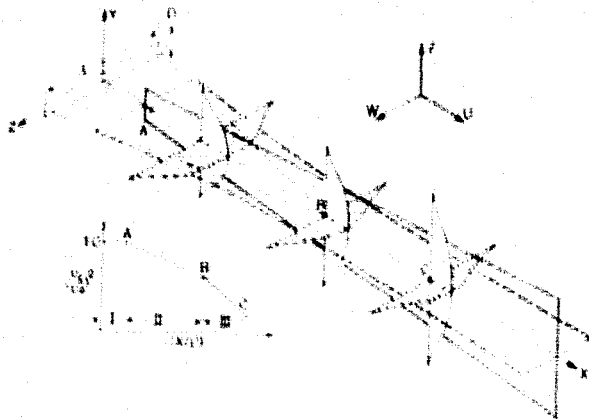


Fig. 2 Schematic Representation of Flow Field of a Rectangular Free Jet

shown in the figure (as an insert) is the variation of $\ln(U_c/U_0)^2$ with $\ln X/D$. The three regions, as shown in the figure, may be classified as follows: the first region is referred to as a potential core region in which the axial velocity is constant; the second region denoted by AB, in which the velocity decays at a rate roughly the same as that of a planar jet, will be referred to as the two-dimensional region; and the third region downstream of B, in which the velocity decays at nearly the same rate as that of an axisymmetric jet will be referred to as an axisymmetric region. The two-dimensional type region originates at about the location where the two shear layers in the X,Y plane (containing the short dimension of the nozzle) meet. Correspondingly, one may expect the axisymmetric region to originate at a location where the two shear layers in the X,Z plane (containing the long dimension of the nozzle) would meet.

Profiles of the mean axial velocity in the X,Y and X,Z planes at three different locations are shown in the schematic of flow structure in Figure 2. In regions I and II, the width of the jet in the X,Z plane is greater, as expected, than the width in the X,Y plane. At B the widths in both planes are about the same. In region III the width in the X,Y plane becomes larger than that in the X,Z plane.

The solid and dashed lines shown in the flow schematic depict the loci of maximum turbulent stresses in the two planes being considered. Detailed discussion of the flow structure with supporting measurements is given by Krothapalli et al. (13).

A schematic of the flow field of a multiple rectangular free jet is shown in Figure 3. Mean velocity

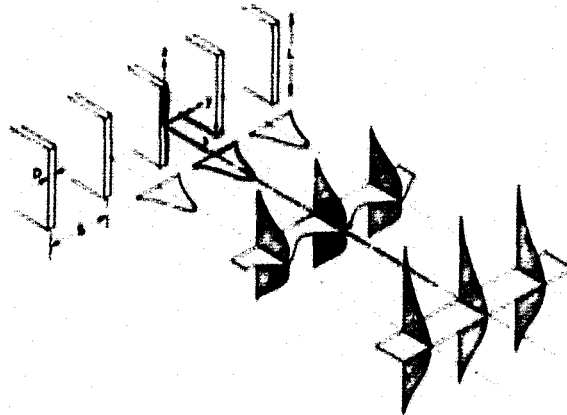


Fig. 3 Schematic Representation of Flow Field of a Multiple Free Jet

profiles in the two central planes for the center three lobes are shown in the figure. For the configuration tested ($S = 8D$, $AR = 16.7$), the flow from each lobe does not exhibit any mutual interaction for X less than $15D$. Complete merging of the jets (i.e., individual jets lose their identity) is observed for X equal to $60D$, as indicated by a flat velocity profile across the lobes. The mean velocity profile in the central X,Z plane at different downstream locations exhibits characteristics similar to that of a single free jet. The shaded region is an attempt to show the pseudo-potential core region, after which the jet acts like a single two-dimensional jet with its minor axis being along the Z-axis.

The confined multiple jet configuration under consideration is shown in Figure 1. The leading edges of the plates are rounded with no fairing added as shown in the figure. The separation distance L_1 between the plates can be varied from 6 cm to 8.5 cm. For L_1 less than 7.5 cm ($L_1 < 1.5L$) low frequency disturbances (characteristic time greater than 1 sec) are found and mean axial velocity profiles (averaging time equal to 1 sec) in the central X,Y plane are found to be asymmetrical about their axes. For L_1 greater than or equal to 7.5 cm ($L_1 \geq 1.5L$), fewer low frequencies were present, and the profiles look very much similar to that of a multiple free jet with some secondary flow induced between the jets. Most of the measurements described hereinafter are for the case of a separation distance of 7.5 cm.

The profiles in the central X,Z plane show marked differences when compared with a multiple free jet configuration, and a schematic of this flow field is shown in Figure 4. The profiles are plotted to scale.

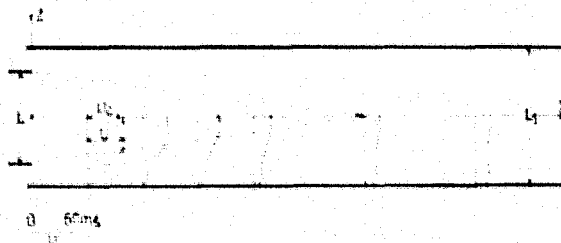


Fig. 4 Schematic of Axial Mean Velocity Profiles in the X,Z Plane of a Multiple Confined Jet

The dotted lines in the figure correspond to a pseudo-potential core where the jet acts like a single jet (see also Figure 3). The end of this pseudo-potential core occurs at X equal to $60D$. For X greater than $60D$, the mean velocity profiles are almost flat across the jet. This observation along with previous discussion (regarding profiles in the X,Y plane) suggest that the mean velocity for X greater than $60D$ is homogeneous.

Mean Velocities

Mean axial velocity profiles, for the case of multiple free jets, in the central X,Y plane for the center three lobes at various downstream locations covering up to X equal to $60D$ are shown in Figure 5. At the exit plane, top half profiles with equal magnitudes are found with very little secondary flow between the jets. Significant merging of the jets

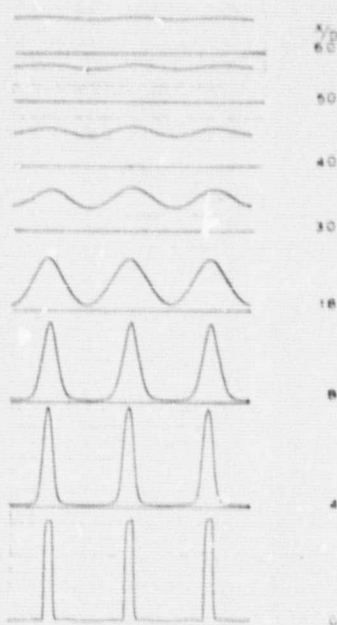


Fig. 5 Axial Mean Velocity Profiles Across the Center Three Jets

first seems to occur at a location of about $18D$. The flat profile establishes that complete mixing of the jets has occurred at a location of approximately $60D$. Velocity profiles are observed to be flat across the center three lobes for locations of $60D \leq X \leq 115D$.

For the configuration ($S = 8D$, $\Delta R = 16.7$) studied, a significant region exists where the mean velocity profiles of the individual jets behave quite independently of each other. However, measurements for the case of two unventilated parallel jets, such as the ones studied by Miller and Cummings (14), show a subatmospheric pressure region between the jets near the nozzle exit and the two jets attract each other. To further examine this phenomenon, a short time exposure ($5 \mu s$) schlieren picture was taken of the three center lobes and is shown in Figure 6. Here, it is observed that the individual jets do not attract each other and mix with ambient air quite independently. The large scale structure which usually appears in the transition region of a jet can be seen in this picture (refer to Krothapalli (7) for details).

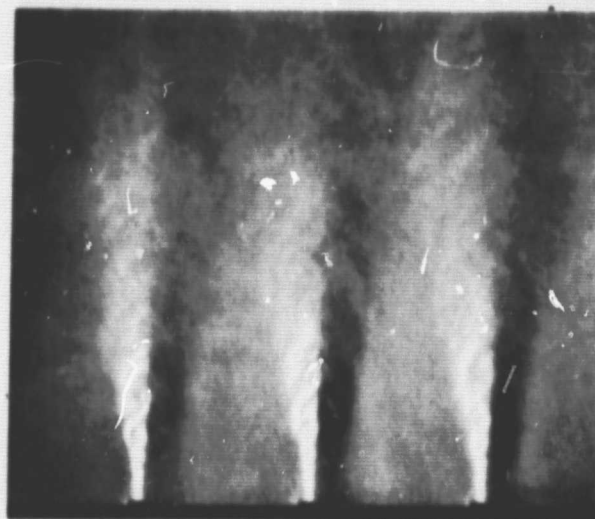


Fig. 6 Schlieren Picture of a Multiple Free Jet

Mean velocity profiles, for the case of multiple confined jets, are observed to be very similar to the ones shown in Figure 5 at their corresponding locations, except in this case, close to the jet exit, a noticeable amount of secondary flow is induced between the jets. The ratio of U_s (secondary flow velocity) to U_0 (exit velocity) is about 0.08 at the exit plane of the nozzle.

The decay of the square of the mean axial velocity with downstream distance for the three cases is shown in Figure 7. The three regions noted in Figure 2 are identified as the potential core region which

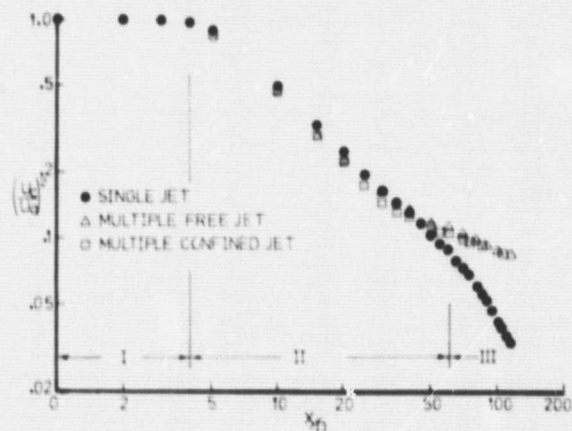


Fig. 7 The Decay of the Axial Mean Velocity Along the Centerline of the Jet

ends at $3D - 4D$, the two-dimensional jet type region extending up to $60D$, and the axisymmetric jet type region extending beyond $60D$. The decay for the case of a multiple free jet is almost identical to a single free jet up to X equal to $40D$. For X greater than $40D$ the decay is slower as shown in the figure. The decay for the case of the multiple confined jet is almost identical to that of a multiple free jet. Judging from this it seems that the effect of the confining surfaces on the centerline velocity of the jet is minimal.

The normalized mean velocity profiles in the X,Y plane for the center jet from $Y = 0$ to $Y = 4D$ (midway between the two adjacent lobes) are shown in Figure 8 for the three cases. The profiles upstream of the

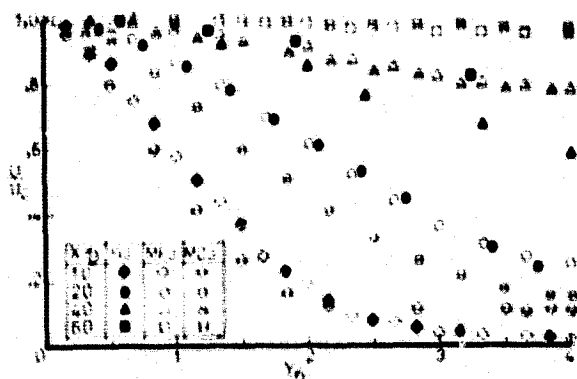


Fig. 8 Axial Mean Velocity Profiles in the X,Y Plane

merging region are identical for the cases of a single jet and the multiple free jet as depicted by the profiles at X equal to $10D$. A nearly flat profile is observed at $60D$. Most of the profiles for the case of the multiple confined jet, for X less than $40D$, have magnitudes less than those of the single and multiple free jets, when compared at their corresponding locations. The secondary flow induced between the jets is first noticed in the profile at X equal to $10D$. For X greater than or equal to $60D$, profiles for the multiple free jet and multiple confined jet are almost identical, as shown in the figure, and the mean velocity is uniform across the lobes.

The normalized mean velocity profiles in the central X,Z plane for the case of the multiple free jet are shown in Figure 9 for various downstream locations. For X less than or equal to $40D$, the profiles

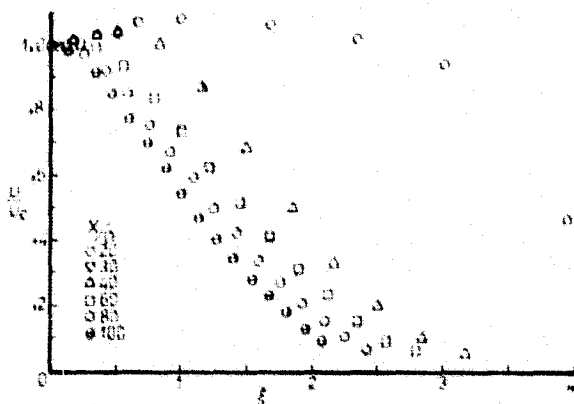


Fig. 9 Axial Mean Velocity Profiles in the X,Z Plane of a Multiple Free Jet

exhibit a saddle shape with a maximum appearing near the centerline, and are identical to that of a single free jet when compared at their corresponding locations. Profiles for X greater than $40D$ in the multiple free jet case are broader than that of a single jet at their corresponding locations. To further examine this, the growth rate in the X,Z plane of the center jet in both the single and multiple free jet configurations are plotted with downstream distance in Figure 10. The growth rate in the X,Y plane for a single jet is also included in the figure (Y_c and Z_c are the distances from the centerline of the jet to a location where the mean velocity is half of the centerline velocity along Y and Z axes respectively).

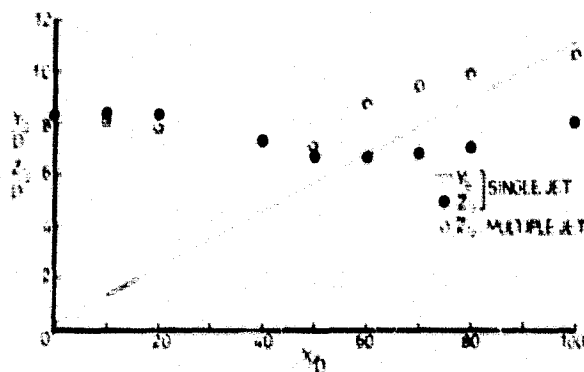


Fig. 10 The Growth of the Jet with Downstream Distance

As one expects from the above discussion, the growth rate of the jet in the X,Z plane for both cases is almost identical up to X equal to $40D$. For X greater than $40D$, the growth rate in the multiple jet configuration is greater than that of a single jet. From these observations it may be concluded that, for the spacing studied, the mutual interaction between the jets is strongly felt at about X equal to $40D$, while significant merging of the jets in the central X,Y plane occurs at X equal to $20D$.

The normalized mean velocity profiles in the X,Z plane for the case of a confined multiple jet are shown in Figure 11. The abscissa Z is normalized with respect to the lobe width D , while as before the mean velocity is normalized with respect to the centerline mean velocity at the corresponding location. The figure also indicates the position of the plate. For X less than or equal to $40D$, the profiles exhibit a saddle shape. For locations X greater than or equal to

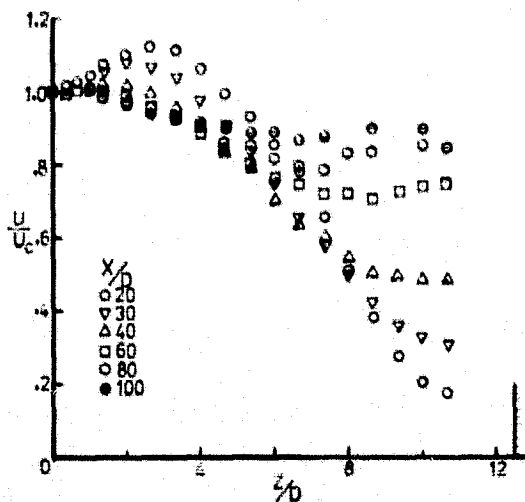


Fig. 11 Axial Mean Velocity Profiles in the X,Z Plane of a Confined Multiple Jet

$60D$, the profiles are more nearly uniform across the jet, and have a local minimum as shown in the figure. These profiles along with the profiles in the central X,Y plane (see Figure 8) for X greater than $60D$ suggest that the mean flow is roughly a uniform flow field.

Turbulent Intensities and Shear Stresses

The rms intensity for the axial component of velocity along the centerline of the jet for each of the three cases is shown in Figure 12, along with the results (data represented by a solid line) of Gutmark and Wygnanski (15) for a planar jet. The rms intensity is normalized with respect to the mean axial velocity at the exit rather than with the local mean

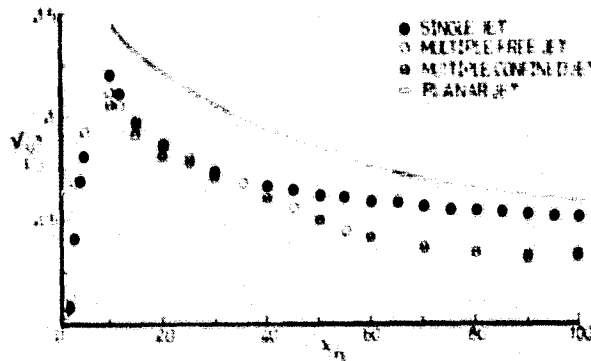


Fig. 12 The Variation of the rms Value of the Axial Component of Velocity Along the Centerline of the Jet

centerline velocity. The rms values are almost identical in all the three cases for X less than $40D$. For X greater than $40D$, the values are almost identical for the multiple free and confined jets, with magnitudes less than that of a single free jet. This substantial reduction in magnitude is the result of a mutual interaction between the adjacent jets. The results for a planar jet are shown for purposes of comparison and exhibit values higher than that of the single rectangular jet. It is felt that this difference can be attributed to different initial conditions in the two experiments.

We have observed that the values of v_{rms} and u_{rms} along the centerline have variations similar to u_{rms} . For X greater than $60D$ we have found $v_{rms} = w_{rms} = 0.9 u_{rms}$ for the case of the multiple free jet and $v_{rms} = 0.88 u_{rms}$ and $w_{rms} = 0.83 u_{rms}$ for the case of the confined multiple jet, which suggest isotropy along the centerline of the jet.

Figure 13 presents the profiles for $\bar{u}(u_{rms}/U_c)$ in the X,Y plane for the case of the multiple free jet and for different downstream locations. Profiles for X less than $20D$ are almost identical to a single free jet when compared at appropriate locations. For X greater than or equal to $60D$, the profiles become flat

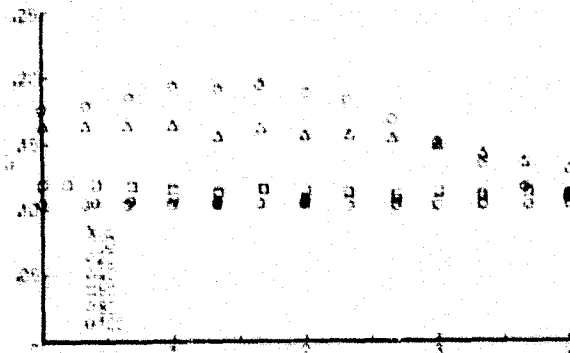


Fig. 13 The Distribution of Axial Velocity Fluctuation in the X,Y Plane of a Multiple Free Jet

just as the mean velocity profiles. It was also found that the profiles of v and w for X greater than or equal to $60D$ are flat and equal in magnitude with u at their corresponding locations. This again suggests isotropy in the central X,Y plane.

To further examine the degree of isotropy in the central X,Y plane, the normalized turbulent shear stress \bar{uv} for different downstream locations are plotted in Figure 14. For X equal to $20D$, the profile is quite similar to that of a single jet. For X

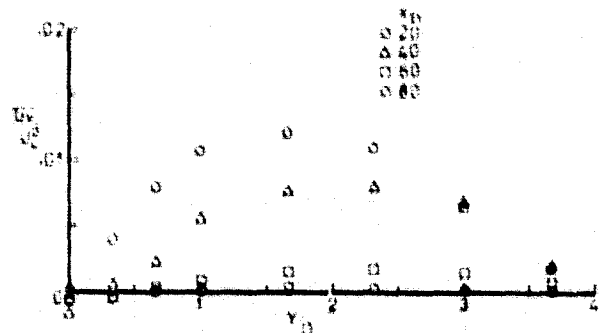


Fig. 14 The Distribution of the Turbulent Shear Stress in the X,Y Plane of a Multiple Free Jet

greater than $60D$, the normalized stress is quite small in contrast to a single jet where it varies only slightly with downstream distance. The normalized turbulent shear stress \bar{uv} in the X,Y plane is found to be negligible for all downstream stations studied.

Similar observations were also made in the case of the confined multiple jet configuration. Reference to these measurements can be found in the report by Krothapalli (7).

The profiles of \bar{u} in X,Z plane, for the case of multiple free jets, and for various downstream locations covering up to $100D$ are shown in Figure 15. For X less than $40D$, the profiles are similar to those for

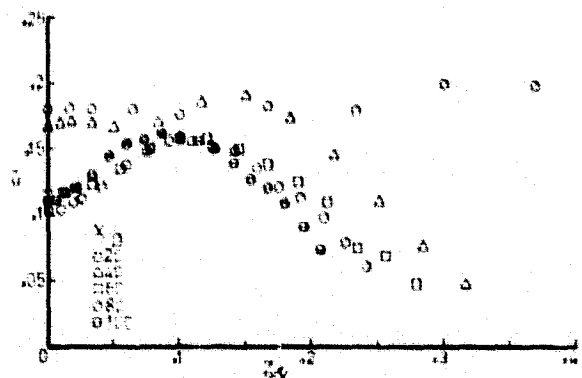


Fig. 15 The Distribution of Axial Velocity Fluctuation in the X,Z Plane of a Multiple Free Jet

a single free jet. For X greater than or equal to $60D$, the profiles develop a pronounced saddle shape as shown in the figure. The appearance of a saddle shape profile in a jet usually indicates the end of the potential core. With this in mind, one may conclude that the flow field appears as though it is emerging from a single two-dimensional slot with the width of the slot being the long dimension of the lobe. The shaded region in Figure 3 was drawn to represent a pseudo-potential core for this equivalent two-dimensional jet which ends at X equal to about $60D$.

The profiles of \bar{u} in the central X,Z plane, in the case of the confined multiple jet, for different downstream locations, are shown in Figure 16. The

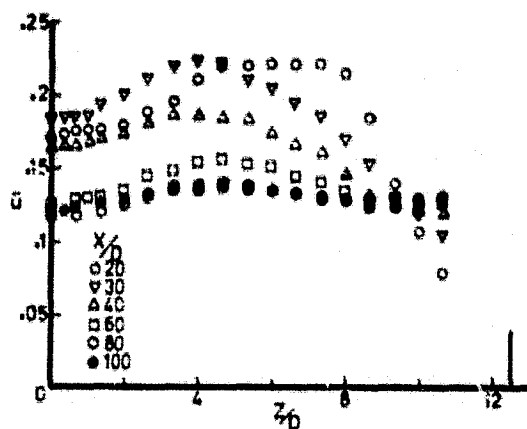


Fig. 16 The Distribution of Axial Velocity Fluctuation in the X,Z Plane of a Confined Multiple Jet

distance along the Z axis is normalized with respect to the width D. Profiles for X less than 20D are almost identical to those of a multiple free jet when compared at corresponding locations. Unlike the previous case, a very mild saddle shape profile is developed at X equal to 60D, and the profile is nearly uniform. Further flattening occurs for locations X greater than 60D. This observation along with the corresponding profiles in X,Y plane suggest that the field of turbulence is quite homogeneous.

We have observed that the profiles of \bar{v} and \bar{w} are also uniform for X greater than 60D, with the values $\bar{v} \approx 0.88\bar{u}$, and $\bar{w} \approx 0.83\bar{u}$. Judging from these results one can conclude that the flow field in the channel for X greater than 60D is nearly homogeneous and isotropic in structure. The flow field for the center three jets thus have characteristics quite similar to that of a flow generated by a grid.

The normalized turbulent shear stress $\bar{u}'\bar{w}'$ in the central X,Z plane, in the case of the multiple free jet are plotted in Figure 17. At each location X, the

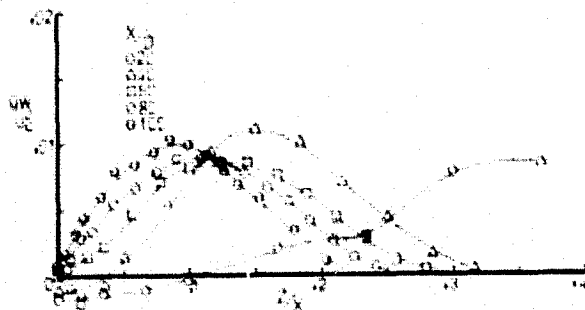


Fig. 17 The Distribution of the Turbulent Shear Stress in the X,Z Plane of a Multiple Free Jet

point of maximum shear stress corresponds to the point where the velocity gradient ($\partial u / \partial z$) and turbulent intensities are maximum. We again found, when compared with that of a single free jet, that the values of $\bar{u}'\bar{w}'$ for X greater than 40D are less at corresponding locations. In addition, the magnitudes of $\bar{u}'\bar{w}'$ are negligible in the central X,Z plane.

The normalized turbulent shear stress $\bar{u}'\bar{w}'$ in the X,Z plane, in the case of a confined multiple jet, for various downstream locations are shown in Figure 18.

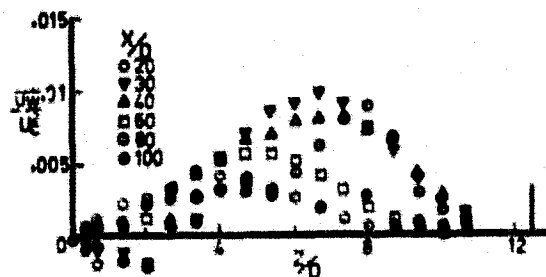


Fig. 18 The Distribution of the Turbulent Shear Stress in the X,Z Plane of a Confined Multiple Jet

The values of $\bar{u}'\bar{w}'$ in the present case are lower than those for the multiple free jet at corresponding locations. The values of $\bar{u}'\bar{w}'/\bar{u}^2$ across the jet for X equal to 100D are very small (of the order of 0.003). Likewise, the magnitudes of $\bar{u}'\bar{w}'$ in X,Z plane are found to be very small.

These results along with mean velocities and turbulent intensities in both X,Y and X,Z planes suggests that the flow field is nearly homogeneous and isotropic in the channel for X greater than 60D.

CONCLUSIONS

In the case of a single rectangular jet, the flow is characterized by the presence of three distinct regions when the decay of the square of the axial mean velocity is used to describe the flow field. These regions are: the potential core region, a two-dimensional type region and an axisymmetric region.

For the case of a ventilated array of rectangular jets having a spacing of 8D the following observations are made. Because the individual jets act quite independently of each other near the nozzle exit, the point at which the individual jets begin to merge can be estimated from data on the growth rate of a single jet. Far downstream the flow field appears as if it is emerging from a single two-dimensional slot with the width of the slot being the long dimension of a single lobe. The mutual interaction between the jets results in a lower turbulence level when compared to a single jet at corresponding locations.

For the case of the confined multiple jet with a separation distance between the plates of 1.5L, the following observations are made. The flow field in the central X,Y plane (plane of the array) was little affected by the presence of the plates and the mean velocity profiles look very much similar to that of the multiple free jet at corresponding locations. For X greater than 60D, the mean velocity profiles are uniform across the lobes (in the X,Y plane) as in the previous case, and in addition the profiles are uniform across the jet in the X,Z plane. The field of turbulence for X greater than 60D was found to be uniform and isotropic in structure. From these observations one may conclude that the flow field, for the configuration under study, and for X greater than 60D, is nearly homogeneous and isotropic.

REFERENCES

1. Corrisin, S., "Investigation of the Behavior of Parallel Two Dimensional Air Jets," *NACA W-90*, 1944.
2. Laurence, C. J., Benninghof, N. J., "Turbulence Measurements in Multiple Interfering Air Jets," *NASA TN 4029*, 1957.
3. Laurence, C. J., "Turbulence Studies of a Rectangular Slotted Noise Suppressor Nozzle," *NASA TND-294*, 1960.

4. Marsters, F. G., "Measurements in the Flow Field of a Linear Array of Rectangular Nozzles," AIAA Paper 79-0350, AIAA 17th Aerospace Science meeting, January 1979.
5. Knystautas, R., "The Turbulent Jet from a Series of Holes in Line," The Aeronautical Quarterly, Vol. XV, February 1964.
6. Aiken, N. T., "Aerodynamic and Noise Measurements on a Quasi-Two Dimensional Augmentor Wing Model with Lobe Type Nozzles," NASA TMX-62,237, September 1973.
7. Krothapalli, A., "An Experimental Study of Multiple Jet Mixing," Ph.D. Dissertation, Stanford University, June 1979.
8. Sforza, M. P., Steiger, H. M., and Trentacoste, N., "Studies on Three Dimensional Viscous Jets," AIAA Journal, Vol. 4, May 1966, pp. 800-806.
9. Trentacoste, N., and Sforza, M. P., "Further Experimental Results for Three-Dimensional Free Jets," AIAA Journal, Vol. 5, May 1967, pp. 885-891.
10. Sfeir, A. A., "The Velocity and Temperature Fields of Rectangular Jets," Int. J. Heat and Mass Transfer, Vol. 19, 1975, pp. 1289-1297.
11. Sfeir, A. A., "Investigation of Three Dimensional Turbulent Rectangular Jets," AIAA 11th Fluid and Plasma Dynamics Conference, 76-1185, July 1978.
12. Rajaratnam, N., Turbulent Jets, Elsevier, New York, 1976, pp. 267-271.
13. Krothapalli, A., Baganoff, D., and Karamcheti, K., "Turbulence Measurements in a Rectangular Jet," AIAA 17th Aerospace Sciences meeting, 79-0074, January 1979.
14. Miller, R. D., Cummings, W. E., "Force Momentum Fields in a Dual Jet Flow," J. Fluid Mechanics, Vol. 7, No. 2, 1960, pp. 237-255.
15. Gutmark, G., and Wygnanski, I., "The Planar Turbulent Jet," J. Fluid Mechanics, Vol. 73, Part 3, 1976, pp. 465-495.